Color-tunable hetero-dinuclear Pt(II)/B(III) and Pt(II)/Ir(III) arrays with N^O-julolidine ligands

Adela Nano,*[,a,†] Maria Pia Gullo,[b] Barbara Ventura,[b] Andrea Barbieri,*[,b] Nicola Armaroli,[b] Raymond Ziessel [a]

[a] Institut de Chimie et Procédés pour l'Énergie, l'Environnement et la Santé (ICPEES), UMR 7515 au CNRS, Ecole Européenne de Chimie, Polymères et Matériaux (ECPM), 25 rue Becquerel, 67087 Strasbourg Cedex 02, FRANCE.

[b] Istituto per la Sintesi Organica e la Fotoreattività (ISOF), Consiglio Nazionale delle Ricerche (CNR), Via P. Gobetti 101, 40129 Bologna BO, ITALY.

KEYWORDS. Julolidine, N^O ligands, Boron(III), Platinum(II), Iridium(III), White light emission.

Supporting Information Placeholder

ABSTRACT: The synthesis and photophysical properties of two multichromophoric systems, Pt(II)/B(III) and Pt(II)/Ir(III), based on novel N^O-julolidine ligands are reported. The functionalization of the julolidine core enables the introduction of two different anchoring sites, a terminal acetylene and a N^O chelating moiety, which allow the assembling of two different chromophoric centers. The complex photophysical behavior of these multicomponent arrays is rationalized by investigating a series of model compounds, which are prepared through specific synthetic pathways. The photophysical properties of the final multicomponent arrays are investigated in parallel with the models. The multichromophoric system, composed by a platinum(II) and an iridium(III) chromophores connected through a modified julolidine ditopic ligand, displays a peculiar excitation wavelength dependent luminescence behavior. It exhibits tuning of the emission color from blue to orange, passing through pure and warm white.

INTRODUCTION

Multichromophoric systems assembling properly selected individual subunits may result in inter-component photo-induced electron transfer (PET) and/or electronic energy transfer (EET) processes, which can lead to efficient directional energy migration and/or charge separation, respectively. The study of such systems provides useful information for the understanding of these fundamental processes, which are highly relevant for artificial photosynthesis,[1-4] information transduction,[5] energy storage,[6-8] and optoelectronic devices,[9-12] particularly in the area of white-light emitters.[13,14]

The majority of white-light emitting materials rely on mixing different luminophores – typically red, green and blue (RGB) – which can uniformly cover the visible spectral window ranging from 400 to 700 nm.[12,15,16] However, the use of individual white emitters may offer remarkable advantages, *e.g.*, better color quality, reproducibility and simpler device fabrication with respect to mixing different compounds.[14,17,18] In this regard, a common strategy entails the use of multichromophoric systems in which partial energy transfer occurs from a donor to one or more acceptors.[19-21] Alternatively, white color can be obtained by the combination of two complementary blue and orange-emitters exhibiting excited state intramolecular proton transfer (ESIPT).[22-24] For instance, in a previous work we have reported the panchromatic luminescence of novel N^O julolidine-based ligands.[23]

Only few examples of dinuclear heterometallic systems bearing Pt(II) and Ir(III) chromophores within the same ligand skeleton have been reported.[25] On the other hand, very limited information about julolidine derivatives exploited as coordinating ligands with transition metals is found in the literature.[26,27] Recently, Borisov *et al.* have reported the synthesis and optical properties of palladium(II) and platinum(II) complexes bearing tetradentate Schiff bases, one being a tetradentate N^O julolidine-based ligand.[28] Due to the conformational rigidity, the electron lone pair of the nitrogen atom of this ligand is fully conjugated within the aromatic π-system, conferring unusual electronic reactivity to the julolidine core. Numerous julolidine-containing organic materials have been reported for applications in biology (*e.g.*, fluorescent molecular rotors)[29] and photonic devices (*e.g.*, OLEDs).[30] They are found to be highly efficient red-emitters due to their tricyclic structure which locks the nitrogen atom. Furthermore, the presence of tetramethyl groups on the scaffold increases the solubility and prevents molecular aggregation in the solid state.

Building upon our previous work on julolidine dyes,[23] herein we describe the incorporation of a platinum(II)

and an iridium(III) or boron(III) center into the julolidine skeleton, thus generating Pt(II)/Ir(III) or Pt(II)/B(III) arrays, respectively. To this end, a chelating N^O site capable of coordinating iridium(III) as well as boron(III) and a terminal alkynyl group able to link a platinum(II) chromophore were introduced within the julolidine core.

RESULTS AND DISCUSSION

Synthesis. The protocols for the synthesis of the related ligands and the relevant Pt(II)/B(III) and Pt(II)/Ir(III) arrays are sketched in Schemes 1 and 2. The pivotal ligand $\mathbf{L_1}$ was synthesized by condensation of julolidinylaldehyde[31-33] and 4-iodoaniline in ethanol in the presence of catalytic amount of *p*-TsOH under reflux, as previously described for anil derivatives.[34,35] The terminal alkyne was introduced by a Sonogashira cross-coupling reaction promoted by Pd(II)/CuI catalysts between $\mathbf{L_1}$ and trimethylsilyl(TMS)-acetylene. A large excess of KF in THF solution was necessary for the deprotection of the TMS group of $\mathbf{L_2}$, thus giving the key arylacetylide $\mathbf{L_3}$ in 76% yield. Complexation of $\mathbf{L_3}$ with the boron difluoride fragment by reaction with $BF_3{\cdot}Et_2O$ in 1,2-dichloroethane (DCE) gave the boranil derivative $\mathbf{BL_3}$ in 94% yield. $\mathbf{BL_3}$ can also be obtained from $\mathbf{BL_1}$ in two steps using similar synthetic methods. However, we noted that it is more difficult to functionalize the iodide after the BF_2 complexation step has occurred.

Scheme 1. Synthetic pathways for compound $\mathbf{L_1}$ to $\mathbf{PtIrL_3}$

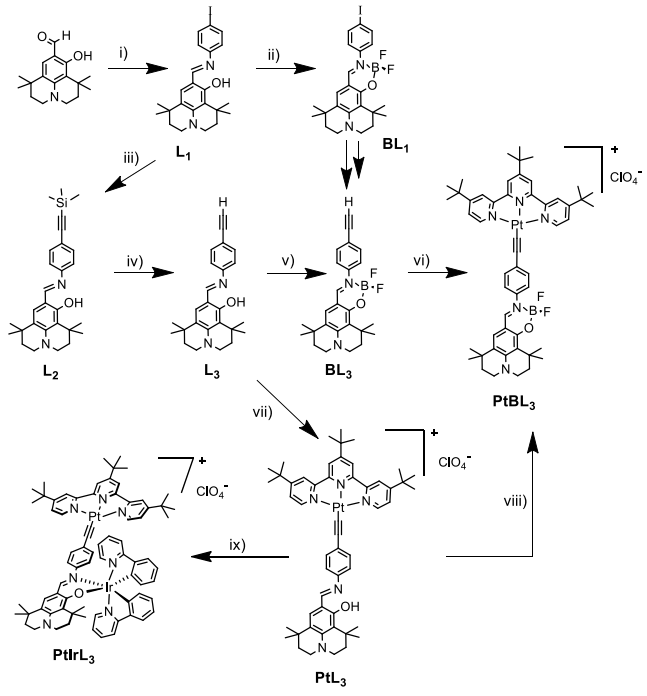

i) 4-iodoaniline, *p*-TsOH cat., dry EtOH, 95°C, 12 hrs, 75%. *ii)* $BF_3{\cdot}Et_2O$ (6 eq.), 1,2-dichloroethane, r.t., 30 min. then DIPEA (6 eq.), 3 hrs, 89%. *iii)* $[Pd(PPh_3)_2Cl_2]$ 10 mol%, CuI 10 mol%, TMS acetylene, $^{i}Pr_2NH$, THF, r.t., 12 hrs, 99%. *iv)* KF (100 eq.), MeOH/H_2O, THF, r. t., 12 hrs, 76%. *v)* $BF_3{\cdot}Et_2O$ (6 eq.), 1,2-dichloroethane, r.t., 30 min.; DIPEA (6 eq.), 3 hrs, 94%. *vi)* $[(^{t}Bu_3tpy)PtCl](BF_4)$, $^{i}Pr_2NH$, THF, CuI, r.t., 12 hrs., than $LiClO_4$, H_2O, DMF, 99%. *vii)* $[(^{t}Bu_3tpy)PtCl](BF_4)$, $^{i}Pr_2NH$, THF, CuI, r.t., 12 hrs., than $LiClO_4$, H_2O, DMF, 70%. *viii)* $BF_3{\cdot}Et_2O$ (2 eq.), 1,2-dichloroethane, r.t., DIPEA (2 eq.), 3 hrs. *ix)* $[(ppy)_2Ir(\mu\text{-}Cl)]_2$, MeOH/1,2-dichloroethane, $^{i}Pr_2NH$, 60°C, overnight, 81%.

Eventually, coupling of $\mathbf{BL_3}$ with $[Pt(^{t}Bu_3tpy)Cl]BF_4$ is achieved under inert atmosphere using CuI as catalyst in the presence of (diisopropyl)amine (DIPA). The reaction gave $\mathbf{PtBL_3}$ as a red powder in quantitative yields after anion exchange with perchlorate salts and purification. An alternative route for the preparation of $\mathbf{PtBL_3}$ is depicted in Scheme 1. This synthetic pathway involves the interaction of $\mathbf{L_3}$ with the $[(^{t}Bu_3tpy)PtCl]BF_4$ precursor in the presence of DIPA and catalytic amounts of CuI yielding first the complex $\mathbf{PtL_3}$. Subsequently, the free chelating N^O site of the latter was coordinated by the boron difluoride entity *via* a reaction with $BF_3{\cdot}Et_2O$ under basic conditions. This is an interesting route because it provides the platinum complex $\mathbf{PtL_3}$ lacking the boron center, which is a useful spectroscopic reference. It has to be noticed that anion exchange (PF_6^- or BF_4^- with ClO_4^-) facilitates the solubility and the purification of the complexes. Finally, coordination of the Ir(III) metal precursor to the chelating N^O site is achieved by reacting $\mathbf{PtL_3}$ with the $[(ppy)_2Ir(\mu\text{-}Cl)]_2$ precursor in a 1,2-dichloroethane/methanol mixture at 60°C (Scheme 1). The hetero-bimetallic complex $\mathbf{PtIrL_3}$ was isolated in 81% yield as a dark fine powder after anion exchange and purification from column chromatography.

Scheme 2. Alternative synthetic pathway for the preparation of $\mathbf{IrL_n}$ (n = 1-3)

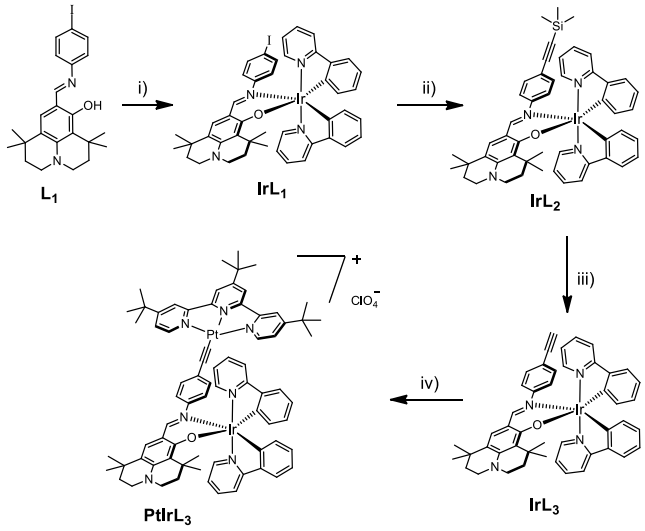

i) $[(ppy)_2Ir(\mu\text{-}Cl)]_2$, MeOH, 1,2-dichloroethane, NEt_3, 80°C, 2 days, 72%. *ii)* $[Pd(PPh_3)_2Cl_2]$ 10 mol%, CuI 10 mol%, TMS acetylene, $^{i}Pr_2NH$, THF, r.t., 12 hrs., 99%. *iii)* KF (100 eq.), THF, MeOH, H_2O, refluxing overnight, 72%. *iv)* $[(^{t}Bu_3tpy)PtCl](BF_4)$, $^{i}Pr_2NH$, THF, CuI, r.t., 12 hrs, 78%.

In order to prepare additional spectroscopic references a second synthetic route was undertaken to enable the preparation of the bimetallic complex **PtIrL$_3$** in four steps (Scheme 2). Metalation of **L$_1$** with the precursor $[(ppy)_2Ir\text{-}(\mu\text{-}Cl)]_2$ is feasible in a MeOH/DCE solution by heating at 80 °C for two days. Interestingly, the conversion of the iodide group to the alkyne function in the **IrL$_1$** complex is accomplished in two steps using standard Sonogashira cross-coupling reaction with TMS-acetylene.[36] The stable **IrL$_3$** derivative was linked to the $[(^tBu_3tpy)PtCl]BF_4$ precursor in THF at room temperature using CuI under anaerobic conditions. The target **PtIrL$_3$** complex was isolated pure in 78% yield by column chromatography, precipitation and several washings with pentane. Recrystallization in adequate solvents afforded the analytically pure samples. All compounds were unambiguously characterized by ^{1}H- and ^{13}C-NMR, ESI-MS, IR-ATR and elemental analysis. They were found to be stable in solution within days also in the presence of light.

Infrared characterization. The IR spectrum of **L$_3$** and **BL$_3$** exhibits a strong absorption around 3,300 and 2,100 cm^{-1} assigned to the ν(Csp-H) and ν(C≡C) stretching vibration, respectively.[23] The ν(Csp-H) band disappears in the platinum complexes **PtL$_3$**, **PtBL$_3$** and **PtIrL$_3$** indicating the metalation of the ligand through the carbon of the acetylene function. Furthermore, this is confirmed by the appearance of a large band at 1,080 cm^{-1} corresponding to the stretching vibration of the perchlorate counter-anion. The IR spectrum of **IrL$_3$** suggests a weaker acetylene ν(C-H) stretching vibration, shifted at lower frequencies by ~50 cm^{-1} compared to that of the free ligand. The absorption band of ν(C=N) appearing at 1,590 cm^{-1} for the free ligand **L$_3$** is shifted to lower frequencies in **IrL$_3$** and **PtIrL$_3$** indicating the coordination of the ligand to the metal center through the nitrogen atom.

NMR characterization. The proton NMR spectra of the ligands **L$_1$**, **L$_2$** and **L$_3$** recorded in $CDCl_3$ show a broad and weak signal at ~14.0 ppm which is assigned to OH proton.[23] This signal is shifted downfield, due to the hydrogen bond that is formed with the free doublet of nitrogen atom. Absence of this peak in the ^{1}H NMR spectra of Pt(II), Ir(III) and B(III) complexes (Figure S3, S5, S7, S9, S11) indicates the deprotonation of OH group and its coordination to the metal or boron center through the oxygen. The singlet at ~8.40 ppm appearing in ligands spectra is assigned to the CH=N proton, which is shifted at 7.70-7.94-ppm upon complexation.

Absorption properties. Selected absorption data for ligands and complexes recorded in CH_3CN solution (c = 10^{-5} M) at room temperature (r.t.) are gathered in Table 1, the relevant spectra are reported in Figure 1 and Figure S13-S15.

All ligands display a broad absorption band at about 400-430 nm (Figure 1, top) with relatively high absorption coefficient (ε_{max} = 40,300 – 64,500 M^{-1}cm^{-1}, Table 1). This band is assigned to $^1\pi,\pi^*$ transitions[37] and is not influenced by solvent polarity. Passing from the open chain to the closed boranil derivatives, it is red shifted by approximately 20 nm and its intensity increases.

The absorption profiles of Pt(II) arrays, **PtL$_3$** and **PtBL$_3$** (Figure 1, bottom) can be described by considering the features of the model compound $[(^tBu_3tpy)Pt\text{-}C{\equiv}C\text{-}Tol]BF_4$ (**Pt**).[38] Moving from higher to lower energies, the envelop of bands below 350 nm can be ascribed to intra-ligand (IL) $^1\pi,\pi^*$ transitions of the alkynyl bridge and of the substituted terpyridine (tpy) ligand.[39,40] In the visible region, the expected mixed Pt→tpy ^{1}MLCT / $\pi(C{\equiv}C) \rightarrow \pi^*$(tpy) LLCT transitions are masked by the intense ligand centered (LC) transitions of the julolidine moiety (λ_{max} = 408 and 428 nm for **PtL$_3$** and **PtBL$_3$**, respectively). The nature of this low energy band is also confirmed by its spectral position and intensity, which is the same of the free ligand, not affected by the presence of the metal. Overall, the absorption spectra of the **PtL$_3$** and **PtBL$_3$** dyads match reasonably well the sum of the spectra of the single model components **Pt**, **L$_3$** and **BL$_3$** (Figure S14). The only exception to an otherwise good superposition is in the presence of a shoulder in the low energy side of the lowest energy absorption band. This discrepancy is attributed to a distortion effect of the electronic cloud, possibly introduced by the metal-ligand interaction. Still, Pt → tpy and Pt → julolidine transitions are reasonably involved and the presence of C≡C → julolidine ILCT transitions cannot be excluded.

The spectra of the complexes **IrL$_1$** and **IrL$_3$** are almost superimposable (Figure 1, bottom) and display two characteristic bands, as reported for the corresponding model $[Ir(ppy)_3]$ (**Ir**).[41,42] The most intense and sharp band, peaking at about 260 nm (ε_{max} = 55,300 and 58,800 M^{-1}cm^{-1}, for **IrL$_1$** and **IrL$_3$** respectively), is assigned to singlet spin allowed ^{1}LC transition, centered on the phenyl-pyridine groups. A second broad and less intense band appears at about 370 nm (ε_{max} = 23,500 and 23,600 M^{-1}cm^{-1}, for **IrL$_1$** and **IrL$_3$**, respectively) and is related to ^{1}CT transition.[43] One should note that the intensity of the characteristic absorption band of **L$_n$** is significantly reduced when coordinated to the $\{Ir(ppy)_2\}$ fragment (Figure S13). The long-wavelength absorption tail above 480 nm is ascribed to the spin-forbidden ^{3}MLCT transition, enhanced by the iridium metal spin-orbit coupling (ζ_{Ir} = 3,909 cm^{-1}).[44] It should be noted that, contrary to what observed for the **PtL$_3$** and **PtBL$_3$** derivatives, the absorption spectra of **IrL$_n$** do not obviously match the spectral sum of **Ir** and **L$_n$**. In fact, these systems cannot be considered as an array of two components, but rather heteroleptic complexes of Ir(III) (Figure S13).

The absorption profile of the multichromphoric system **PtIrL$_3$** (Figure 1, bottom) is consistent with the sum

of its own model components **Pt** and **IrL$_3$** (Figure S15), suggesting the presence of a weak electronic coupling between the individual units. Moving from higher to lower energy, it is possible to observe two sets of bands,as in the Ir(III) models, and to recognize the distinct contributions of the single components. The specific features are listed below: (*i*) the most intense band, up to 350 nm, is typical of $^1\pi,\pi^*$ tpy/ppy centered transitions ($\lambda_{max} \approx 260$ nm), (*ii*) the broad mixed Ir(III) and Pt(II) ^{1}MLCT/^{1}LLCT transition band, extended from 350 to 500 nm; (*iii*) the ^{3}MLCT band originating from the spin-forbidden direct transition to the lowest triplet state, appearing as a tail with low intensity up to 600 nm.

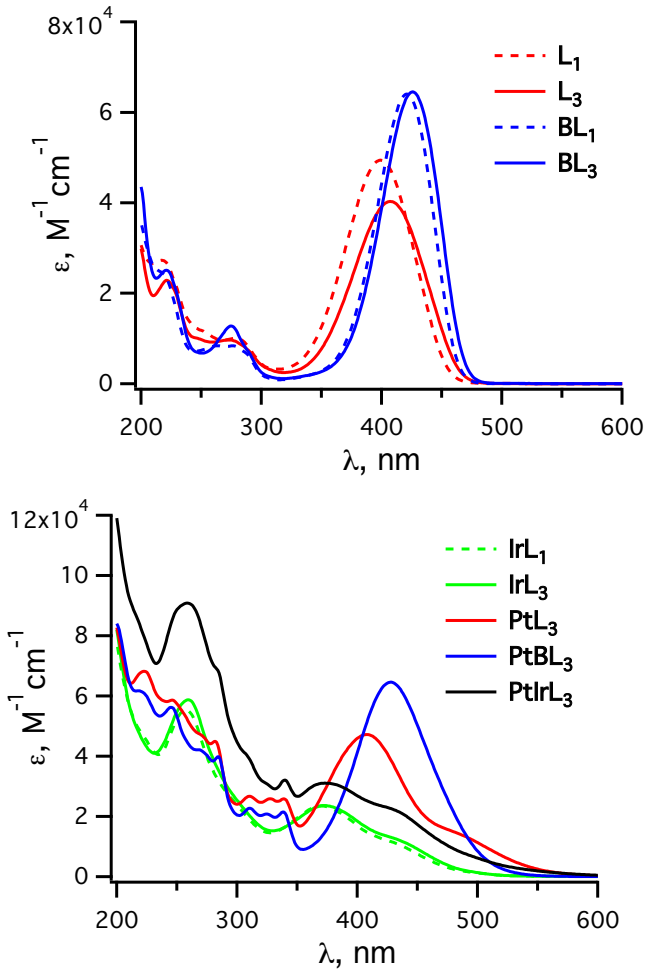

Figure 1. Absorption spectra of ligands **L$_1$**, **L$_3$**, **BL$_1$** and **BL$_3$** (top) and complexes **IrL$_1$**, **IrL$_3$**, **PtL$_3$**, **PtBL$_3$** and **PtIrL$_3$** (bottom) in CH_3CN solution at r.t.

Table 1. Absorption features of compounds [a]

	λ_{max}, nm ($\varepsilon_{max} \times 10^{-3}$, $M^{-1}cm^{-1}$)
L$_1$ [b]	217 (27.1), 279 (10.0), 399 (49.0)
L$_3$ [b]	221 (22.9), 273 (9.7), 407 (40.3)
BL$_1$ [b]	221 (23.5), 265 (8.3), 421 (64.0)
BL$_3$ [b]	221 (25.1), 275 (12.8), 426 (64.5)
Ir	241 (50.2), 280 (48.2), 373 (12.6)
IrL$_1$	257 (55.3), 370 (23.5)
IrL$_3$	260 (58.8), 373 (23.6)
Pt [c]	280 (34.6), 327 (18.9), 440 (2.6)
PtL$_3$	223 (68.3), 310 (26.7), 339 (25.9), 408 (47.2)
PtBL$_3$	245 (56.3), 310 (22.7), 338 (21.5), 428 (64.6)
PtIrL$_3$	258 (92.9), 340 (32.7), 373 (31.4)

[a] In CH_3CN solution at room temperature. [b] Data from ref. 23. [c] Data from ref. 38.

Luminescence properties. All ligands **L$_1$**, **L$_3$**, **BL$_1$** and **BL$_3$**, and Ir(III) complexes **IrL$_1$** and **IrL$_3$**, are luminescent in liquid (Figure 2) and frozen (Figure 3) solutions. The two Pt(II) derivatives **PtL$_3$** and **PtBL$_3$**, and the **PtIrL$_3$** multichromophoric system display emission only at 77 K in glassy matrix (Figure 3), although a faint emission from the latter has been detected at r.t. in de-aerated CH_3CN solution (Table 2). The emission spectra of the iodide derivatives **L$_1$**, **BL$_1$** and **IrL$_1$** are almost superimposable to the parent ethynyl-substituted compounds.

The boranil derivatives **BL$_1$** and **BL$_3$** display the highest values for the luminescence quantum yield ($\phi = 0.75$, Table 2), as expected for the presence of the borate chelation.[37] At low temperature, in frozen solution, they show an intense blue-shifted fluorescence (peaking at about 460 nm) and a weak but clearly detectable phosphorescence emissions ($\lambda_{max} = 584$ and 572 nm, $\tau = 17.1$ and 38.4 ms for **BL$_1$** and **BL$_3$**, respectively), from the lowest triplet excited state (Table 2 and Figure 3, top). **BL$_1$** phosphorescence is shorter-lived than **BL$_3$**, because of the presence of the iodine substituent that promotes the $T_1 \rightarrow S_0$ spin forbidden deactivation ($\zeta_I = 5{,}069$ cm^{-1}).[44] The proton bridged ligands **L$_1$** and **L$_3$** display a dual luminescence in solution at room temperature due to an excited state intramolecular proton transfer process (ESIPT).[23] At low temperature they show a more complex behavior displaying a panchromatic emission from a variety of excited states. The peculiar luminescence features of the ligands **L$_{1,3}$** and **BL$_{1,3}$** have been discussed in a recent communication.[23]

The Ir(III) complexes **IrL$_1$** and **IrL$_3$** display a weak emission at about 580 nm in solution at r.t., that is strongly affected by the presence of oxygen (Table 2). On the basis of the excited state lifetimes measured in air-equilibrated and de-aerated solution a more definite quantification of the oxygen quenching effect has been determined applying the Stern-Volmer analysis. In this case, one can make use of the Stern-Volmer equation to obtain the bimolecular quenching rate constant, k_q:[45]

$$\frac{\tau_0}{\tau} = 1 + k_q \tau_0 [O_2]$$

where, τ_0 is the unquenched lifetime (measured in de-aerated acetonitrile solution), τ is the lifetime in the

presence of the quencher, *i.e.* O_2 (measured in air-equilibrated solution), and $[O_2]$ = 1.9 mM is the oxygen concentration for an air-saturated acetonitrile solution.[44] Using the lifetime values reported in Table 2 we obtain for both Ir(III) complexes **IrL$_1$** and **IrL$_3$** a rather high oxygen quenching rate constant $k_q \approx 1.6 \times 10^{10}$ $M^{-1}s^{-1}$, close to the diffusion controlled limit in that solvent, $k_d = 1.9 \times 10^{10}$ $M^{-1}s^{-1}$.[44]

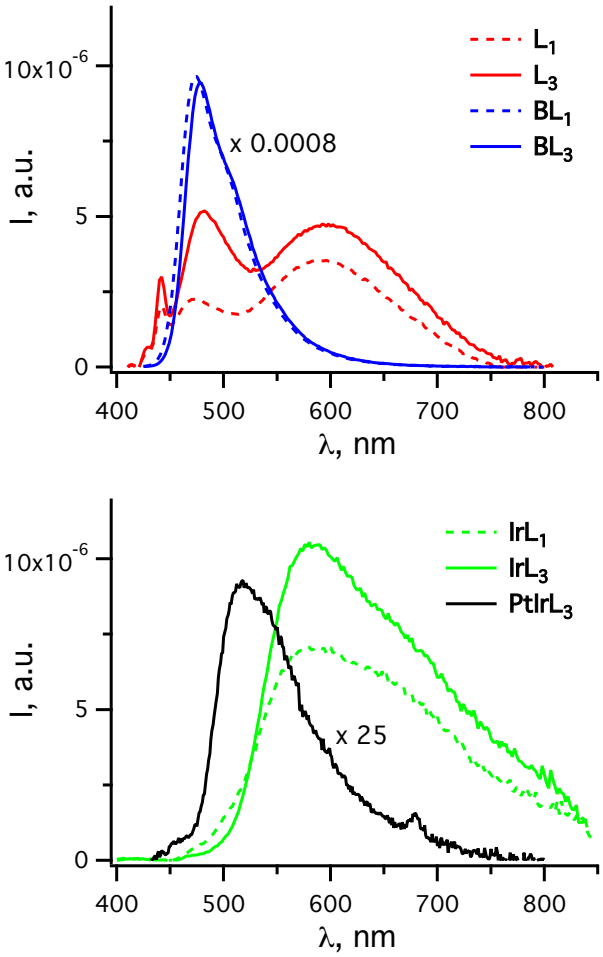

Figure 2. Corrected emission spectra of ligands **L$_1$**, **L$_3$**, **BL$_1$** and **BL$_3$** (top) and complexes **IrL$_1$**, **IrL$_3$** and **PtIrL$_3$** (bottom) in CH_3CN solution at r.t.; all spectra are rescaled for the relevant quantum yields.

The luminescence properties of **IrL$_1$** and **IrL$_3$** could be attributed to a ^{3}CT nature of the emitting state, as confirmed by the blue shift (1,250 – 1,425 cm^{-1}) of the luminescence maxima on going from solution to glassy matrix. A different assumption might be inferred by the structured emission profile observed at low temperature and from the values of radiative constants ($k_r = \phi / \tau$) in de-aerated solution ($k_r = 2.6 \times 10^3$ and 2.5×10^3 s^{-1}, for **IrL$_1$** and **IrL$_3$**, respectively), *i.e.* ca. 2 orders of magnitude lower than that expected for a neat ^{3}MLCT transition, suggesting a substantial contribution of the ^{3}LC states on the nature of the emission.[43] Thus, it can be concluded, that the emitting excited state has a mixed ^{3}MLCT/^{3}LC character, as often observed for Ir(III) cyclometalated complexes.[43]

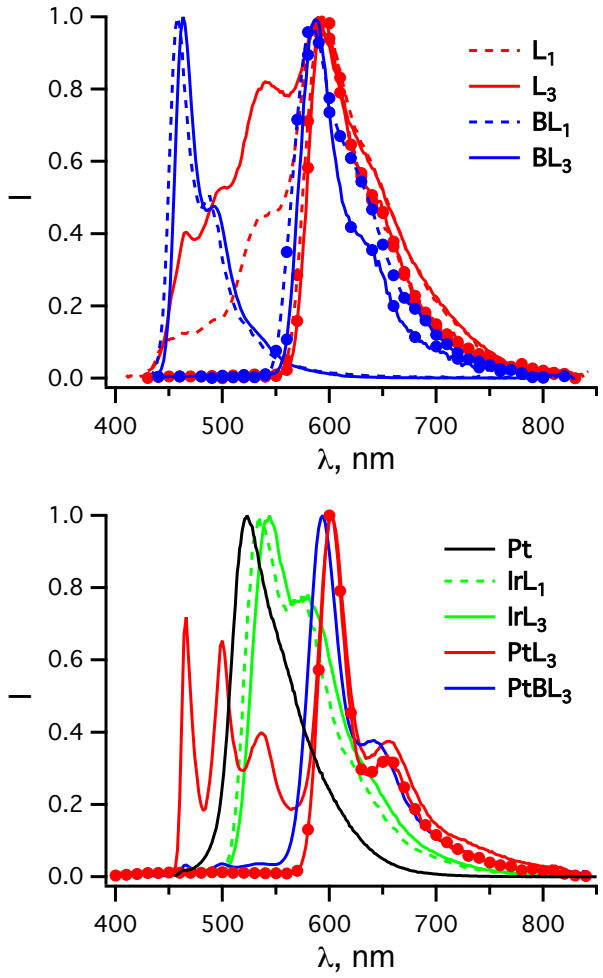

Figure 3. Corrected and intensity normalized emission spectra of ligands **L$_1$**, **L$_3$**, **BL$_1$** and **BL$_3$** (top) and complexes **Pt**, **IrL$_1$**, **IrL$_3$**, **PtL$_3$** and **PtBL$_3$** (bottom) in CH_3OH:C_2H_5OH 1:4 mixtures at 77 K; phosphorescence spectra obtained in gate detection mode (line + symbol).

The introduction of the julolidine unit in its proton bridged or closed form linked to the Pt(II) moiety in the **PtL$_3$** and **PtBL$_3$** arrays completely quenches the typical intense luminescence of the **Pt** center in de-aerated solution at r.t.[38,46] In glassy matrix at 77 K instead, the luminescence spectra of the Pt(II) derivatives display features very similar to the phosphorescence of the ligands, with additional bands at higher energy, more intense in the case of **PtL$_3$** (Figure 3, bottom). From the comparison of the emission profiles of the arrays **PtL$_3$** and **PtBL$_3$** with those of the corresponding models **L$_3$** and **BL$_3$**, recorded with pulsed excitation and gated detection to isolate the longer-lived phosphorescence emission, it is possible to assign the bands peaking at about 600 nm to the triplet excited state of the julolidine moiety (Figure 3). For both arrays, the lifetime values of the emitting triplet excited state are much shorter than those in the free ligands (τ = 0.6 and 3.0 ms for **PtL$_3$** and 0.9 and

3.7 ms for **PtBL$_3$**, Table 2), because of the much faster $T_1 \rightarrow S_0$ non-radiative deactivation induced by the presence of the Pt heavy atom (ζ_{Pt} = 4,481 cm^{-1}).[44] The data are well fitted by a bi-exponential decay function (χ^2 = 0.9940 and 1.1822 for **PtL$_3$** and **PtBL$_3$**, respectively), even though a more complex lifetime distribution due to the formation of aggregates in the glassy matrix cannot be excluded. As mentioned, **PtL$_3$** also displays a structured emission starting at about 500 nm (τ = 11.5 μs, Table 2), which is present in **PtBL$_3$** as well with similar energy and lifetime (Table 2). By comparison with the features of the **Pt** model (Table 2), it can be attributed mainly to ^{3}MLCT transitions.[40] The emission band observed at λ = 466 nm (τ < 0.02 ns, Table 2) in the spectrum of **PtL$_3$** (Figure 3, bottom) occurs at about the same wavelength as for **L$_3$** (Figure 3, top). This has been attributed to a residual fluorescence from the enolic (E) and the keto (K) forms of the proton bridged julolidine moiety because of the ESIPT process.[23] Indeed, a similar band is absent in **PtBL$_3$** which bears the closed form of julolidine. Thus, the emission observed for the Pt(II) derivatives mainly originates from excited states located on the julolidine ligand.

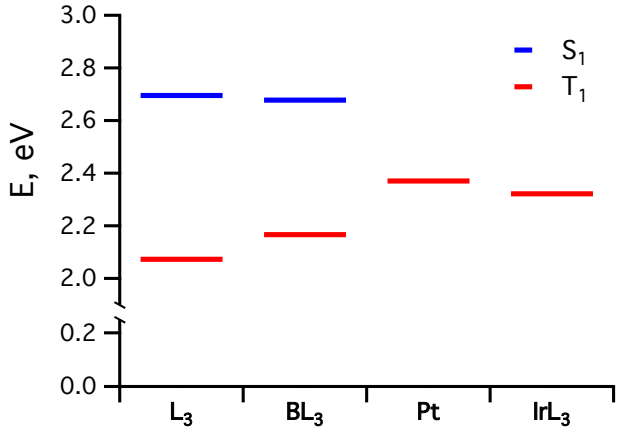

Figure 4. Excited-state energy level diagram with the ground state set as zero.

The emission features of the complexes in solution at r.t. can be rationalized taking into account the energy level diagram sketched for these systems and reported in Figure 4. The energy of the excited states has been estimated from fluorescence (S_1), when available, and phosphorescence (T_1) emission maxima at 77 K of the models **L$_3$**, **BL$_3$**, **Pt** and **IrL$_3$**. As already discussed above, in the section on the absorption properties, these represent good models for the relevant **PtL$_3$**, **PtBL$_3$** and for **PtIrL$_3$** arrays. From the diagram reported in Figure 4 it is clear that the triplet excited state of the julolidine ligands, both in its open (**L$_3$**) or closed (**BL$_3$**) form, lies at lower energy with respect to the Pt- and Ir-based triplet excited state. Giving the CT nature of the lowest energy excited states assessed for the **PtL$_3$**, **PtBL$_3$** and **PtIrL$_3$** complexes, it is thus possible to assume that an almost complete energy transfer process occurs from the Pt- to the julolidine-based triplet state, which is non-emissive at r.t.. As a consequence, the emission originating from the Pt(II) component is almost completely quenched by the presence of the julolidine moiety, that acts as an energy sink for the system. On the other hand, the Ir(III) derivatives **IrL$_1$** and **IrL$_3$** still display a weak emission of mixed CT/LC character, which might be explained by the LC contribution to the nature of the excited state with respect to the Pt(II) analogues.

In the case of the multichromophoric system, **PtIrL$_3$**, only a faint emission is detected at r.t. (λ_{max} = 518 nm, ϕ = 3.5 × 10^{-5} in de-aerated solution, Table 2 and Figure 2), which can be rationalized by the same arguments provided for the interpretation of the emission features of the Pt(II) and Ir(III) metal complexes reported above. On the other hand, at 77 K **PtIrL$_3$** shows a peculiar behavior displaying a wavelength dependent broad and multi-peak emission that covers the whole visible range, with contribution from all constituent moieties. In order to unravel the contribution of the individual units, the emission and the excitation spectra at different excitation and emission wavelengths have been recorded as emission maps. Selected spectra are reported in Figure 5 and the relevant emission/excitation map is shown in Figure S16. It should be noted that even exciting almost selectively the ligand and metal units, it was not possible to pinpoint the contribution from the individual components.

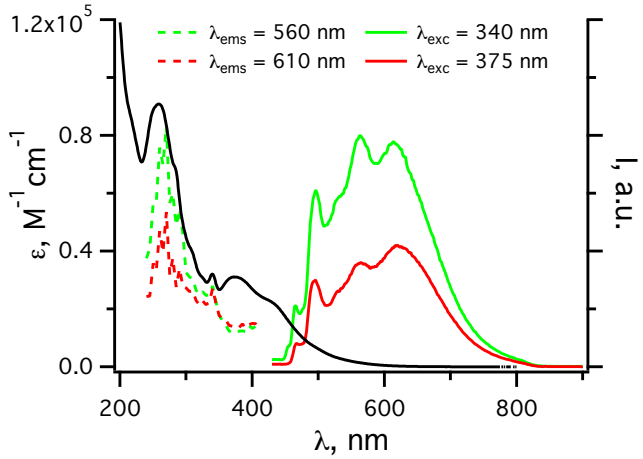

Figure 5. Emission (full lines), excitation (dashed lines) and absorption (black line) spectra at selected wavelengths of **PtIrL$_3$** in CH_3OH:C_2H_5OH 1:4 mixtures at 77 K.

Thus, in order to unravel the origin of the emissions, time resolved luminescence spectra have been recorded. By applying the global analysis to the kinetic traces at different emission wavelengths, the decay associated spectra (DAS) have been obtained. These represent the spectra that would be obtained if the components were isolated and then measured individually. The DAS obtained upon excitation at 370 nm, together with the relevant steady-state spectrum at the same excitation wave-

length are reported in Figure 6. Here, one can observe contributions of three species, with different spectral shapes and lifetimes (λ_{max} = 500, 560, 630 nm and τ = 4.6, 11.8 μs, 1.1 ms, respectively). By comparison with the spectral features of the **PtL$_3$**, **PtBL$_3$** and **IrL$_3$** models (Table 2), the high-energy emission (Figure 6, blue line) can be attributed to the Pt(II)-based ^{3}CT excited state. Similarly, the DAS peaking at 560 nm (Figure 6, green line) has a spectral shape and a lifetime that remind those of **IrL$_3$** (Table 2). The low-energy component (Figure 6, red line), can be attributed to the ^{3}LC states based on the julolidine ligand. The contribution of the latter species to the overall luminescence appears depressed, as also evidenced from the comparison between the time-resolved (Figure 6, full black line) and steady state (Figure 6, dashed black line) luminescence spectra. This is due to the different sensitivity of our TCSPC apparatus with respect to the fluorimeter above 600 nm.

Overall, this kind of behavior highlights the panchromatic nature of the **PtIrL$_3$** emitter, as already observed for the ligands **L$_1$** and **L$_3$**,[23] possibly induced by an incomplete energy transfer from metal-based excited states to the relevant ^{3}LC states. A precise estimation of the efficiency of such processes cannot be performed because of the low emission intensity recorded for **PtIrL$_3$** in the different regions of interest. However, it should be noted that, as a consequence of the limited efficiency of the energy transfer processes in the multichromophoric system **PtIrL$_3$**, the emission spectra observed in the glassy matrix at 77 K are dependent on the excitation wavelength (Figure 5).

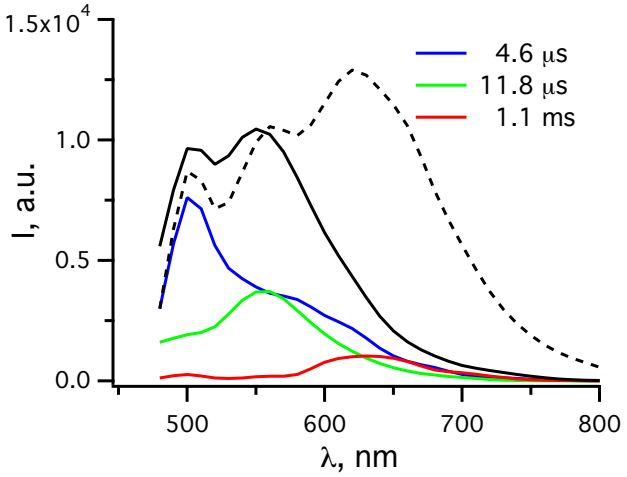

Figure 6. Decay associated spectra (blue, green and red lines) from the time-resolved luminescence of **PtIrL$_3$** in CH_3OH:C_2H_5OH 1:4 mixtures at 77 K. The sum of the components (full black line) and the steady-state emission (dashed black line) are reported for comparison; the relevant lifetime components are indicated in the legend.

Table 2. Luminescence features of compounds

	rt [a]			77 K [b]	
	λ_{max}, nm	ϕ	τ, ns	λ_{max}, nm	τ, μs
L$_1$	470	0.7×10^{-3} (0.7×10^{-3})	< 0.02	460	1.12×10^{-3}
	600		0.12	594	11.6×10^{3}
L$_3$	480	1.1×10^{-3} (1.1×10^{-3})	< 0.02	multipeak	1.33×10^{-3}
	600		0.13	598	54.6×10^{3}
BL$_1$	473	0.74 (0.82)	1.91 (2.01)	458	1.87×10^{-3}
				584	17.1×10^{3}
BL$_3$	479	0.75 (0.80)	1.89 (1.97)	463	1.84×10^{-3}
				572	38.4×10^{3}
IrL$_1$	578	0.4×10^{-3} (2.8×10^{-3})	30.8 (1,140)	534	10.6
IrL$_3$	584	0.5×10^{-3} (3.4×10^{-3})	34.5 (1,310)	544	11.2
Pt [c]	605	4.7×10^{-3} (13.0×10^{-3})	313 (920)	523	20.0
PtL$_3$	n.d.	n.d.	n.d.	466	$< 0.02\times10^{-3}$
				500	11.5
				600	0.6×10^{3}, 3.0×10^{3} (50:50)
PtBL$_3$	n.d.	n.d.	n.d.	500	11.3
				594	0.9×10^{3}, 3.7×10^{3} (70:30)
PtIrL$_3$	518	n.d. (3.5×10^{-5})	n.d.	multipeak	multiexponential

[a] In air-equilibrated (de-aerated) CH_3CN solution at rt. [b] In CH_3OH:CH_2Cl_2 glass at 77 K. [c] Data from ref. 38. For quantum yield: λ_{exc} = 400 nm for **L$_1$** and **L$_3$**, 420 nm for **BL$_1$** and **BL$_3$**, 330 nm for **IrL$_1$** and **IrL$_3$**, and 340 nm for **PtIrL$_3$**. For lifetime: λ_{exc} = 373 nm for **L$_1$**, **L$_3$**, **BL$_1$** and **BL$_3$**, 331 and 370 nm for **PtL$_3$**, **PtBL$_3$**, **IrL$_1$**, **IrL$_3$** and **PtIrL$_3$**. n.d. is not detected.

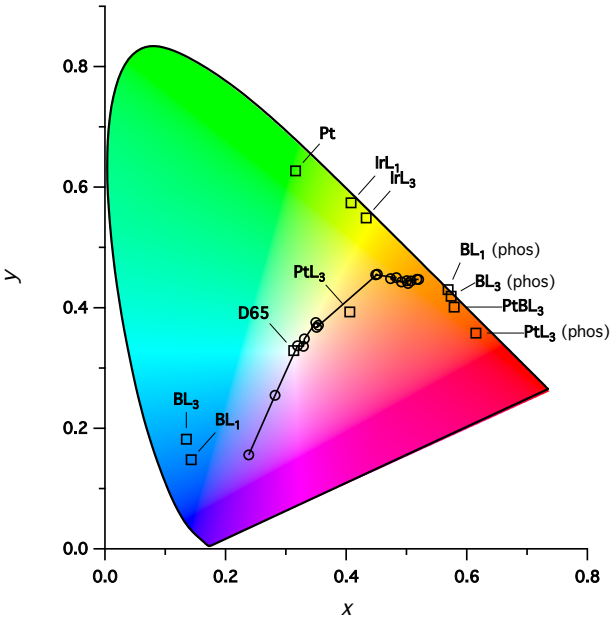

Figure 7. CIE 1931 spectral chromaticity coordinates of luminescence from **BL_1**, **BL_3** ligands and **Pt**, **IrL_1**, **IrL_3**, **$PtBL_3$** complexes (hollow squares), and of the **$PtIrL_3$** array at different excitation wavelengths, λ_{ex} = 240-410 nm (hollow circles) in CH_3OH:C_2H_5OH (1:4) mixture at 77 K. D65 is the standard illuminant for noon daylight.

The color coordinates in the CIE 1931 color space have been calculated at different excitation wavelengths, in the range 240-410 nm, from the relevant irradiance spectra. The results are reported in Figure 7, together with the color coordinates obtained for the **BL_1** and **BL_3** ligands, both from fluorescence and phosphorescence emissions, and for the Pt(II) and Ir(III) metal complexes prepared. For excitation wavelengths between 260 and 280 nm, the color coordinates calculated for the **$PtIrL_3$** luminescence clearly show white emission comparable to that of the CIE standard illuminant **D65** (0.313, 0.329) corresponding to noon daylight.[47] At longer excitation wavelengths (290-310 nm) a slightly warmer white can be obtained (0.35, 0.37).

CONCLUSION

The introduction onto julolidine dyes of an N^O chelating site, capable to coordinate iridium(III) as well as boron(III), and of a terminal alkynyl group, which can graft a platinum(II) chromophore, has allowed the synthesis of a series of luminescent metal complexes and arrays. The peculiar properties of the **BL_n** derivatives, in particular their high quantum yields, arise from the rigidification of the N^O julolidine backbone by boron(III) complexation. In the multichromophoric arrays, the photophysical investigation has unearthed an interplay of ^{3}CT and ^{3}LC excited states, based on the specific transition metals and the julolidine ligands, respectively. This has resulted, in the **$PtIrL_3$** multichromophoric system, in a remarkable excitation wavelength dependent emission of the **$PtIrL_3$** array that has allowed the generation of pure and warm white color in glassy matrix at 77 K.

EXPERIMENTAL SECTION

General Procedures and Materials. All reactions, except those indicated, were performed under a dry atmosphere of argon. [(^{t}Bu$_3$tpy)PtCl]BF_4,[48] [(ppy)$_2$Ir-(μ-Cl)]$_2$,[42] [Pd(PPh_3)$_2Cl_2$],[49] Julolidine[50] were prepared according to literature. The (trimethylsilyl)acetylene, copper iodide, 2-phenylpyridine (ppy) and 4-iodoaniline were purchased from Sigma Aldrich and used as purchased. THF was distilled from sodium and benzophenone under un argon atmposphere. 1,2-dichloroethane was distillated from P_2O_5 under an argon atmosphere. ^{1}H NMR (300, 400 MHz) and ^{13}C NMR (75, 100 MHz) spectra were recorded at room temperature in $CDCl_3$, C_6D_6 or CD_3CN in a Bruker Advance spectrometer. Chemical shifts for ^{1}H and ^{13}C NMR were reported to the delta scale in ppm relative to the residual signals of the deuterated used solvent as internal standards. The 128 MHz ^{11}B NMR spectra were recorded at room temperature with B in borosilicate glass as internal references. Chromatographic purifications were performed using 40-63 μm silica gel (SiO_2) or deactivated aluminum oxide (Al_2O_3 + 6% H_2O weight) 90 standardized. The Infrared spectra were recorded as solid samples on a Perkin Elmer Spectrum One equipped with ATR diamond apparatus. Mass spectra were measured with a JEOL JMS-T100 LO Acc TOF (ESI-MS). Elemental analysis was conducted by an Elementar Vario MICRO Cube apparatus. All samples were dried under high vacuum during 24 h prior to elemental analysis.

The synthesis of ligands **L_1** , **L_3**, **BL_1** and **BL_3** has been described in a previous paper.[23]

Compound PtL_3: ^{i}Pr_2NH (1 mL) was added to a solution of **L_3** (25 mg, 0.067 mmol) and [(^{t}Bu$_3$tpy)$_3$PtCl]BF_4 (48 mg, 0.067 mmol) in THF (5mL). After stirring 10 minutes at room temperature, a small pearl of CuI was added to the solution under an atmosphere of argon and the mixture was continued stirring at room temperature overnight. After evaporation of the solvents, the crude was dissolved in DMF (5 mL) and added dropwise to a stirring solution of lithium perchlorate ($LiClO_4$) (285 mg, 2.68 mmol) in water (15 mL). Finally, the mixture was stirred at room temperature for an additional hour and filtered through a filter paper. The crude was purified over a deactivated aluminum oxide column chromatography, eluting with CH_2Cl_2/MeOH to give the title compound as a brown powder (50 mg, 70 %). ^{1}H NMR ($CDCl_3$, 400 MHz) δ: 1.23 (s, 6H), 1.36 (s, 18H), 1.49-1.52 (m, 2H), 1.59 (s, 9H), 1.66-1.68 (m, 2H), 1.78 (s, 6H) 2.82-2.88 (m, 4H), 6.44 (d, *J* = 6.0 Hz, 2H), 6.91 (s, 1H), 6.96 (s, 1H), 7.36 (s, 1H), 7.95 (d, *J* = 8.3, 2H), 8.18 (s, 1H, -C*H*N), 8.63 (s, 2H), 8.66 (s, 2H), 8.91 (d, *J* = 6.0 Hz, 2H), 14.7 (s, 1H, -O*H*); ^{13}C NMR ($CDCl_3$, 100 MHz) δ:28.4, 29.7, 30.2, 30.4, 30.5, 31.8, 32.3, 36.3,

36.5, 37.5, 39.9, 47.1, 47.5, 97.7, 104.7, 109.3, 114.6, 120.6, 120.8, 121.6, 121.9, 122.7, 123.0, 123.2, 123.3, 124.9, 125.5, 125.6, 128.3, 129.7, 132.9, 133.0, 146.6, 147.4, 151.0, 153.9, 154.0, 154.2, 158.4, 158.8, 160.7, 160.8, 167.3, 167.9, 168.3, 168.4; DEPT ($CDCl_3$, 100 MHz) positive (CH_3, CH) δ: 28.4, 30.2, 30.4, 30.5, 30.9, 120.6, 121.6, 123.0, 123.1, 125.0, 125.4, 128.3, 132.9, 154.0, 160.7 negative (CH_2) δ: 36.3, 40.0, 47.0, 47.5; IR-ATR (cm^{-1}) ν: 608, 621, 727, 841, 1080, 1197, 1312, 1614, 1668, 1723, 2916, 2958; MS-ESI dichloromethane + methanol 9/1: *m/z* (intensity, nature of the peak) 967.3 (100, $[M\text{-}ClO_4]^+$); Anal. calc. for $C_{52}H_{62}ClN_5O_5Pt$: C, 58.50; H, 5.85; N, 6.56. Found: C, 58.32; H, 5.64; N, 6.27.

Compound $PtBL_3$: $^{i}Pr_2NH$ (1 mL) was added to the solution of $\mathbf{BL_3}$ (20 mg, 0.047 mmol) and $[(^{t}Bu_3tpy)_3PtCl]BF_4$ (34 mg, 0.049 mmol) in THF (5mL). After 10 minutes under stirring at room temperature, a small pearl of CuI was added to the solution under an argon atmosphere and the mixture was continued stirring at room temperature overnight. After evaporation of the solvents, the crude was dissolved in a small volume of DMF (2 mL). Afterwards, a solution of lithium perchlorate (200 mg, 1.880 mmol) in water (13 mL) was added dropwise to the DMF solution of the crude under continuous stirring. The mixture was stirred for an additional hour at room temperature and filtered through a filter paper. The crude was purified over a deactivated aluminum oxide column chromatography, eluting with CH_2Cl_2/EtOH 1 % to give the desired product as a red powder in 99% yield. ^{1}H NMR ($CDCl_3$, 400 MHz) δ: 1.27 (s, 6H), 1.40 (s, 9H), 1.51 (s, 18H), 1.58 (s, 6H), 1.71-1.72 (m, 2H), 1.78-1.82 (m, 2H), 3.31-3.35 (m, 2H), 3.39-3.43 (m, 2H), 7.11-7.19 (m, 5H), 7.65-7.76 (m, 2H), 7.94 (s, 1H), 8.16-8.17 (m, 2H), 8.21 (s, 2H), 9.16 (d, ^3J = 6.0 Hz, 2H); ^{13}C NMR ($CDCl_3$, 100 MHz) δ: 28.3, 29.7, 29.8, 30.3, 30.4, 30.4, 31.8, 32.0, 35.4, 36.4, 37.1, 39.0, 47.4, 47.9, 53.4, 101.5, 104.4, 107.4, 114.3, 121.4, 122.4, 122.9, 125.3, 125.7, 128.3, 132.7, 141.3, 151.4, 153.7, 157.5, 157.9, 158.8, 166.5, 167.2 ^{11}B NMR (CD_3CN, 128 MHz) δ: 0.92 (t, $J_{B\text{-}F}$ = 17.6 Hz); IR-ATR (cm^{-1}) ν: 622, 843, 1084, 1209, 1312, 1501, 1584, 1618, 2109 (-C≡C-, vw), 2959; MS-ESI dichloromethane + methanol 9/1: *m/z* (intensity, nature of the peak) 1015.4 (100, $[M\text{-}ClO_4]^+$); Anal. calc. for $C_{52}H_{61}BClF_2N_5O_5Pt$: C, 55.99; H, 5.51; N, 6.28 found: C, 55.74; H, 5.21; N, 6.04.

Compound IrL_1: To the suspension of $[(ppy)_2Ir\text{-}(\mu\text{-}Cl)]_2$ (145 mg, 0.14 mmol) in MeOH (1mL) and 1,2-dichloroethane (4 mL), $\mathbf{L_1}$ (80 mg, 0.17 mmol) and NEt_3 (71 µL, 0.51 mmol) were added. The mixture was placed at 80 °C during 2 days. After it had been cooled down to ambient temperature, dichloromethane was added and the organic phase was washed with water. The organic layer was dried over hydrophilic cotton and concentrated under vacuum. The crude was purified by precipitation in a CH_2Cl_2/MeOH mixture giving $\mathbf{IrL_1}$ as an orange powder (118 mg, 72 %). ^{1}H NMR ($CDCl_3$, 400 MHz) δ: 0.63 (s, 3H), 1.19 (s, 3H), 1.20 (s, 3H), 1.23 (s, 3H), 1.48-1.57 (m, 2H), 1.68 (t, ^3J = 5.8 Hz, 2H), 2.93-3.04 (m, 2H), 3.12 (t, ^3J = 5.8 Hz, 2H), 5.94 (d, J = 8.4 Hz, 2H), 6.19 (d, J = 7.5 Hz, 1H), 6.33 (d, J = 7.5 Hz, 1H), 6.53 (t, ^3J = 7.2 Hz, 1H), 6.60 (t, ^3J = 7.2 Hz, 1H), 6.68-6.72 (m, 2H), 6.82 (t, ^3J = 7.5 Hz, 1H), 6.98 (d, ^3J = 8.4 Hz, 2H), 7.00-7.07 (m, 2H), 7.11 (d, J = 7.6 Hz, 1H), 7.51-7.54 (m, 2H), 7.58-7.67 (m, 2H), 7.70 (s, 1H), 7.81 (d, J = 8.0 Hz, 1H), 8.85-8.89 (m, 2H); ^{13}C NMR ($CDCl_3$, 100 MHz) δ: 27.5, 28.5, 31.1, 31.2, 31.6, 32.1, 36.9, 40.6, 47.2, 47.4, 87.6, 113.1, 117.5, 117.6, 118.3, 119.3, 119.8, 120.6, 120.9, 121.5, 123.2, 123.6, 125.3, 128.7, 128.9, 131.0, 132.7, 133.0, 136.0, 136.1, 144.3, 145.1, 147.6, 148.5, 149.7, 152.6, 153.4, 159.2, 164.7, 168.7, 169.5; DEPT ($CDCl_3$, 100 MHz) CH_3, CH positive mode δ: 27.5, 28.5, 31.1, 31.2, 117.6, 118.3, 119.3, 120.6, 120.9, 121.5, 123.2, 123.6, 125.3, 128.7, 128.9, 131.1, 132.7, 133.0, 136.0, 136.1, 148.5, 149.7, 159.2, negative mode (CH_2) δ: 36.9, 40.6, 47.2, 47.4; IR-ATR (cm^{-1}) ν: 488, 728 vs, 753, 1003, 1183, 1308, 1422, 1475, 1564, 2849, 2920, 3039; MS-ESI dichloromethane + methanol 9/1: *m/z* (intensity, nature of the peak) 975.2 (100, $[M+H]^+$); Anal. calc. for $C_{45}H_{42}IIrN_4O$: C, 55.49; H, 4.35; N, 5.75. Found: C, 55.38; H, 4.18; N, 5.72.

Compound IrL_2: $\mathbf{IrL_1}$ (70 mg, 0.07 mmol), $[Pd(PPh_3)_2Cl_2]$ (18 mg, 0.01 mmol) and CuI (1.5 mg, 0.01 mmol) were placed in a THF (5 mL) solution before addition of $^{i}Pr_2NH$ (0.5 mL) and (trimethylsilyl)acetylene (26 µL, 0.18 mmol) under an argon flow. The reaction media was stirred at room temperature overnight followed by evaporation of the solvent and purification of the crude by using a deactivated aluminum oxide column chromatography (activated with 6 % of water, w/w), and eluting with petroleum ether/CH_2Cl_2: 8/2, v/v. The desired compound was obtained in 99% yield as an orange powder. ^{1}H NMR (C_6D_6, 400 MHz) δ: 0.17 (s, 9H), 1.05 (s, 3H), 1.17 (s, 3H), 1.18 (s, 3H), 1.27-1.31 (m, 2H), 1.40 (t, ^3J = 5.9 Hz, 2H), 1.58 (s, 3H), 2.66-2.81 (m, 4H), 6.21 (t, ^3J = 6.7 Hz, 1H), 6.26 (d, ^3J = 8.3 Hz, 2H), 6.31 (t, ^3J = 6.7 Hz, 1H), 6.55-6.66 (m, 3H), 6.72 (d, ^3J = 7.3 Hz, 1H), 6.77-6.86 (m, 4H), 6.89 (t, ^3J = 7.6 Hz, 1H), 6.94 (d, ^3J = 8.2 Hz, 1H), 6.97 (d, ^3J = 8.3 Hz, 1H), 7.09 (d, ^3J = 8.3 Hz, 2H), 7.35 (d, ^3J = 8.2 Hz, 1H), 7.50 (d, ^3J = 7.4 Hz, 1H), 7.76 (s, 1H), 8.89 (d, ^3J = 5.5 Hz, 1H), 8.96 (d, ^3J = 5.5 Hz, 1H); ^{13}C NMR (C_6D_6, 100 MHz) δ: 0.01, 28.1, 29.1, 31.2, 31.7, 32.6, 37.1, 41.2, 47.3, 93.4, 106.2, 113.9, 117.7, 118.0, 118.2, 118.8, 119.8, 120.4, 120.7, 121.2, 121.3, 123.7, 123.9, 124.1, 129.3, 129.4, 131.3, 131.5, 133.2, 133.6, 135.7, 135.9, 144.5, 145.4, 148.1, 148.4, 149.7, 153.0, 153.7, 153.8, 159.3, 165.2, 169.1, 169.9; IR-ATR (cm^{-1}) ν: 728 vs, 753, 1003, 1182, 1308, 1422, 1475, 1565, 2824, 2916, 3039; MS-ESI dichloromethane + methanol 9/1: *m/z* (intensity, nature of the peak) 945.2 (100, $[M+H]^+$), 872.3 (30, [M-

$Si(CH_3)_3+H]^+$); Anal. calc. for $C_{50}H_{51}IrN_4OSi$: C, 63.60; H, 5.44; N, 5.93. Found: C, 63.42; H, 5.18; N, 5.77.

Compound IrL_3: The solution of **IrL_2** (68 mg, 0.037 mmol) and KF (100 eq.) in a mixture of THF (8 mL), MeOH (2 mL) and water (0.5 mL) was refluxed overnight. Afterwards, the solvents were removed under vacuum and the crude was solubilized in dichloromethane, neutralized with aqueous HCl (2M) and washed several times with water. The organic phase was dried under hydrophilic cotton and evaporated under vacuum. Purification of the product by column chromatography on deactivated Al_2O_3, eluting with petroleum ether/CH_2Cl_2: 7/3, v/v giving **IrL_3** as a deep orange powder (45 mg, 72 %). ^{1}H NMR (C_6D_6, 400 MHz) δ: 1.05 (s, 3H), 1.18 (s, 3H), 1.19 (s, 3H), 1.38-1.42 (m, 2H), 1.53-1.60 (m, 5H); 2.64 (s, 1H), 2.67-2.82 (m, 4H), 6.20-6.24 (m, 3H), 6.29-6.32 (m, 1H), 6.55 (m, 1H), 6.60 (td, ^3J = 7.2 Hz, ^4J = 1.3 Hz, 1H), 6.66 (td, ^3J = 7.2 Hz, ^4J = 1.3 Hz, 1H), 6.72 (m, 1H), 6.77-6.91 (m, 5H), 6.93-6.97 (m, 2H), 7.00 (d, ^3J = 8.4 Hz, 2H), 7.35 (d, ^3J = 8.3 Hz, 1H), 7.51 (d, ^3J = 7.6 Hz, 1H), 7.76 (s, 1H), 8.89 (d, ^3J = 5.5 Hz, 1H), 8.96 (d, ^3J = 5.5 Hz, 1H); ^{13}C NMR (C_6D_6, 100 MHz) δ: 27.9, 28.9, 31.0, 31.4, 32.4, 36.9, 41.0, 47.1, 76.9, 83.8, 113.6, 117.4, 117.5, 117.8, 118.0, 119.5, 120.1, 120.5, 120.9, 121.1, 123.4, 123.6, 123.8, 129.1, 131.1, 131.3, 133.0, 133.4, 135.6, 144.2, 145.1, 147.2, 147.9, 149.4, 152.8, 153.5, 153.6, 156.0, 164.9, 168.8, 169.6; IR-ATR (cm^{-1}) ν: 728, 753, 824, 1029, 1193, 1308, 1475, 1568, 1604, 2106 (C≡C, vw), 2843, 2920, 3037, 3285 (Csp-H, vw); MS-ESI dichloromethane + methanol 9/1: *m/z* (intensity, nature of the peak) 873.2 (100, $[M+H]^+$); Anal. calc. for $C_{47}H_{43}IrN_4O$: C, 64.73; H, 4.97; N, 6.42 found: C, 64.50; H, 4.66; N, 6.30.

Compound $PtIrL_3$: To the suspension of $[(ppy)_2Ir(\mu\text{-}Cl)]_2$ (20 mg, 0.02 mmol) and **PtL_3** (40 mg, 0.04 mmol) in a MeOH (2 mL) and 1,2-dichloroethane (6 mL) mixture, ^{i}Pr$_2$NH was added and the mixture was stirred at 60 °C overnight. After evaporation of the solvents, the crude was dissolved in a small volume of DMF (2 mL). Afterwards, a solution of lithium perchlorate (200 mg, 1.880 mmol) in water (13 mL) was added dropwise to the DMF solution of the crude under continuous stirring. The mixture was stirred for an additional hour and filtered through a filter paper. The crude was purified by column chromatography on deactivated Al_2O_3, eluting with CH_2Cl_2/MeOH 5% to give **$PtIrL_3$** as dark fine powder (53 mg, 81%). ^{1}H NMR (CD_3CN, 400 MHz) δ: 0.58 (s, 3H), 1.16 (s, 3H), 1.20 (s, 3H), 1.21 (s, 3H), 1.45 (s, 19H), 1.51-1.55 (m, 11H), 1.65 (t, ^3J = 5.8 Hz, 2H), 2.93-3.04 (m, 2H), 3.14 (t, ^3J = 5.8 Hz, 2H), 6.14-6.19 (m, 2H), 6.31 (d, ^3J = 8.3 Hz, 1H), 6.45 (t, ^3J = 7.2 Hz, 1H), 6.55 (t, ^3J = 7.2 Hz, 1H), 6.64 (t, ^3J = 7.2 Hz, 1H), 6.79 (t, ^3J = 7.2 Hz, 1H), 6.84 (d, ^3J = 8.2 Hz, 2H), 6.89 (s, 1H), 7.17-7.23 (m, 2H), 7.26 (d, ^3J = 7.6 Hz, 1H), 7.54 (dd, ^3J = 6.0 Hz, ^4J = 1.8 Hz, 2H), 7.60 (d, ^3J = 7.8 Hz, 1H), 7.67-7.73 (m, 2H), 7.80 (t, ^3J = 7.9 Hz, 1H), 7.87 (s, 1H), 7.96 (d, ^3J = 7.8 Hz, 1H), 8.36 (s, 1H), 8.36 (s, 1H), 8.39 (s, 2H), 8.77 (d, ^3J = 6.0 Hz, 2H), 8.80 (d, ^3J = 5.7 Hz, 1H), 8.97 (d, ^3J = 5.7 Hz, 1H); ^{13}C NMR (CD_3CN, 100 MHz) δ: 27.0, 28.1, 29.3, 29.7, 30.2, 30.3, 31.3, 31.8, 36.1, 36.7, 37.1, 40.4, 46.6, 47.0, 54.2, 113.1, 118.6, 119.2, 119.9, 120.7, 121.4, 122.0, 123.2, 123.6, 125.8, 128.3, 128.5, 130.7, 131.6, 132.2, 133.1, 136.9, 137.0, 144.8, 145.6, 147.7, 148.0, 149.9, 152.4, 152.7, 153.6, 153.8, 154.1, 158.8, 159.8, 164.1, 167.0, 167.5, 168.6, 169.1; IR-ATR (cm^{-1}) ν: 556 s, 729, 755, 835 (vs, br), 1030, 1192, 1309, 1422, 1476, 1573, 1605, 1662 vw, 1729 vw, 2922 w; MS-ESI dichloromethane + methanol 9/1: *m/z* (intensity, nature of the peak) 1467.3 (100, $[M\text{-}ClO_4]^+$); Anal. calc. for $C_{74}H_{77}ClIrN_7O_5Pt$: C, 56.71; H, 4.95; N, 6.26 found: C, 56.81; H, 5.28; N, 6.48.

Photophysics. Absorption spectra of dilute CH_3CN solutions (c = 10^{-5} M) were obtained with a Perkin-Elmer Lambda 950 UV/Vis/NIR spectrophotometer. Steady-state photoluminescence spectra were measured using an Edinburgh FSP920 fluorimeter, equipped with the Xe900 Xenon light source and the Peltier-cooled R928P (200-850 nm) Hamamatsu photomultiplier tube (PMT). Phosphorescence spectra were measured using the μF 920H Xenon flashlamp as pulsed light source and the R928P PMT in gated detection mode (freq. 100 Hz, delay 2 ms, gate 6 ms). Luminescence quantum yields (ϕ) at room temperature were evaluated by comparing wavelength integrated intensities (I) of the corrected emission spectra with reference to $[Ru(bpy)_3]Cl_2$ (ϕ_r = 0.028 in air-equilibrated water) and quinine sulphate (ϕ_r = 0.546 in air-equilibrated ethanol) standards,[44] by using the following equation:

$$\phi = \phi_r \frac{I}{I_r}\frac{A_r}{A}\frac{n^2}{n_r^2}$$

where A and A_r are the absorbance values at the employed excitation wavelength, and n and n_r are the refractive indexes of the solvents, respectively for the investigated and the reference compound. The concentration was adjusted to obtain absorbance values $A \leq 0.1$ at the excitation wavelengths for room temperature measurements and $0.1 \leq A \leq 0.2$ for low temperature measurements. Oxygen-free samples were obtained by bubbling the solutions for 10 min with a stream of Argon in custom gas-tight fluorescence cells. Band maxima and relative luminescence intensities are obtained with uncertainties of 2 nm and 20 %, respectively. Luminescence lifetimes were obtained using an IBH 5000F single-photon counting apparatus equipped with a TBX Picosecond Photon Detection Module and NanoLED pulsed excitation sources (excitation wavelengths: 373 nm for ligands, **L_1** and **L_3**, **BL_1** and **BL_3**, 331 nm for **IrL_1**, **IrL_3**, **PtL_3**, **$PtBL_3$** and **$PtIrL_3$**) and ps laser source (excitation wavelengths: 407 nm, for **L_1** and **L_3**, **BL_1** and **BL_3**) in CH_3CN solution. In time resolved luminescence experiments, the wavelength dependence of the individ-

ual kinetic components, obtained by global analysis, was plotted through decay associated spectra (DAS). Analysis of luminescence decay profiles against time was accomplished using the Decay Analysis Software DAS v6.5 provided by the manufacturer. The lifetime values were obtained with an estimated uncertainty of 10%. Luminescence measurements of CH_3OH:C_2H_5OH (1:4) frozen glassy solutions at 77 K were conducted by employing quartz capillary tubes immersed in liquid nitrogen, and hosted within homemade quartz cold finger dewar. Luminescence lifetimes at 77 K were obtained using both SpectraLED (excitation wavelengths: 370 nm for ligands, $\mathbf{L_1}$ and $\mathbf{L_3}$, $\mathbf{BL_1}$ and $\mathbf{BL_3}$) and NanoLED excitation sources (331 nm for $\mathbf{IrL_1}$, $\mathbf{IrL_3}$, $\mathbf{PtL_3}$, $\mathbf{PtBL_3}$ and $\mathbf{PtIrL_3}$).

ASSOCIATED CONTENT

Supporting Information. ^{1}H- and ^{13}C-NMR, absorption and emission spectra. The Supporting Information is available free of charge on the ACS Publications website.

AUTHOR INFORMATION

Corresponding Authors

*E-mail: anano@caltech.edu (A.N.), andrea.barbieri@isof.cnr.it (A.B.), to whom correspondence should be addressed.

Present Addresses

† Division of Chemistry and Chemical Engineering, California Institute of Technology (Caltech), Pasadena, California, 91125, USA.

Author Contributions

The manuscript was written through contributions of all authors. All authors have given approval to the final version of the manuscript.

Funding Sources

No competing financial interests have been declared.
Centre National de la Recherche Scientifique (CNRS), IMRA Europe S.A.S., Photonics for Health, Energy and Environment PHEEL (CNR), Bilateral Scientific Cooperation Projects CNR/CONICET, CNR/CNRS-L and CNR/ASRT (CNR), Flagship Project Nanomax N-CHEM (MIUR).

ACKNOWLEDGMENT

Financial support from CNRS, the Italian CNR (project Photonics for Health, Energy and Environment PHEEL, Bilateral Cooperation Projects CNR/CONICET, CNR/CNRS-L and CNR/ASRT-ET) and Italian MIUR (Flagship Project Nanomax N-CHEM) is acknowledged. We are grateful to IMRA Europe S.A.S. (Sophia Antipolis, France) for awarding a PhD fellowship to AN. We thank Drs. Stephane Jacob and Gilles Dennler (IMRA Europe) for many helpful and fruitful discussions.

REFERENCES

(1) Concepcion, J. J.; House, R. L.; Papanikolas, J. M.; Meyer, T. J. Chemical Approaches to Artificial Photosynthesis. *Proc. Natl. Acad. Sci. U. S. A.* **2012**, *109*, 15560-15564.

(2) Gust, D.; Moore, T. A.; Moore, A. L. Realizing Artificial Photosynthesis. *Faraday Discuss.* **2012**, *155*, 9-26.

(3) Tachibana, Y.; Vayssieres, L.; Durrant, J. R. Artificial Photosynthesis for Solar Water-Splitting. *Nat. Photonics* **2012**, *6*, 511-518.

(4) Wen, F. Y.; Li, C. Hybrid Artificial Photosynthetic Systems Comprising Semiconductors as Light Harvesters and Biomimetic Complexes as Molecular Cocatalysts. *Accounts Chem. Res.* **2013**, *46*, 2355-2364.

(5) Norsten, T. B.; Branda, N. R. Axially Coordinated Porphyrinic Photochromes for Non-Destructive Information Processing. *Adv. Mater.* **2001**, *13*, 347-349.

(6) Bozdemir, O. A.; Erbas-Cakmak, S.; Ekiz, O. O.; Dana, A.; Akkaya, E. U. Towards Unimolecular Luminescent Solar Concentrators: Bodipy-Based Dendritic Energy-Transfer Cascade with Panchromatic Absorption and Monochromatized Emission. *Angew. Chem.-Int. Edit.* **2011**, *50*, 10907-10912.

(7) Liu, J. Y.; Yeung, H. S.; Xu, W.; Li, X. Y.; Ng, D. K. P. Highly Efficient Energy Transfer in Subphthalocyanine-BODIPY Conjugates. *Org. Lett.* **2008**, *10*, 5421-5424.

(8) Ziessel, R.; Ulrich, G.; Elliott, K. J.; Harriman, A. Electronic Energy Transfer in Molecular Dyads Built Around Boron-Ethyne-Substituted Subphthalocyanines. *Chem.-Eur. J.* **2009**, *15*, 4980-4984.

(9) Cocchi, M. In *Organic Light-Emitting Diodes*; Buckley, A., Ed. 2013, p 293-318.

(10) Costa, R. D.; Orti, E.; Bolink, H. J.; Monti, F.; Accorsi, G.; Armaroli, N. Luminescent Ionic Transition-Metal Complexes for Light-Emitting Electrochemical Cells. *Angew. Chem.-Int. Edit.* **2012**, *51*, 8178-8211.

(11) Evans, R. C.; Douglas, P.; Winscom, C. J. Coordination Complexes Exhibiting Room-Temperature Phosphorescence: Evaluation of their Suitability as Triplet Emitters in Organic Light Emitting Diodes. *Coord. Chem. Rev.* **2006**, *250*, 2093-2126.

(12) Sasabe, H.; Kido, J. Multifunctional Materials in High-Performance OLEDs: Challenges for Solid-State Lighting. *Chem. Mat.* **2011**, *23*, 621-630.

(13) Frobel, M.; Schwab, T.; Kliem, M.; Hofmann, S.; Leo, K.; Gather, M. C. Get It White: Color-Tunable AC/DC OLEDs. *Light-Sci. Appl.* **2015**, *4*, e247.

(14) Reineke, S.; Thomschke, M.; Lussem, B.; Leo, K. White Organic Light-Emitting Diodes: Status and Perspective. *Rev. Mod. Phys.* **2013**, *85*, 1245-1293.

(15) Lin, Y.-C.; Karlsson, M.; Bettinelli, M. Inorganic Phosphor Materials for Lighting. *Top. Curr. Chem.* **2016**, *374*, 21.

(16) Ying, L.; Ho, C. L.; Wu, H. B.; Cao, Y.; Wong, W. Y. White Polymer Light-Emitting Devices for Solid-State Lighting: Materials, Devices, and Recent Progress. *Adv. Mater.* **2014**, *26*, 2459-2473.

(17) Bolink, H. J.; De Angelis, F.; Baranoff, E.; Klein, C.; Fantacci, S.; Coronado, E.; Sessolo, M.; Kalyanasundaram, K.; Gratzel, M.; Nazeeruddin, M. K. White-Light Phosphorescence Emission from a Single Molecule: Application to Oled. *Chem. Commun.* **2009**, 4672-4674.

(18) Kim, S. H.; Park, S.; Kwon, J. E.; Park, S. Y. Organic Light-Emitting Diodes with a White-Emitting Molecule: Emission Mechanism and Device Characteristics. *Adv. Funct. Mater.* **2011**, *21*, 644-651.

(19) Coppo, P.; Duati, M.; Kozhevnikov, V. N.; Hofstraat, J. W.; De Cola, L. White-Light Emission from an Assembly Comprising Luminescent Iridium and Europium Complexes. *Angew. Chem.-Int. Edit.* **2005**, *44*, 1806-1810.

(20) Praveen, V. K.; Ranjith, C.; Armaroli, N. White-Light-Emitting Supramolecular Gels. *Angew. Chem.-Int. Edit.* **2014**, *53*, 365-368.

(21) Sykes, D.; Tidmarsh, I. S.; Barbieri, A.; Sazanovich, I. V.; Weinstein, J. A.; Ward, M. D. d -> f Energy Transfer in a Series of Ir-

III/Eu-III Dyads: Energy-Transfer Mechanisms and White-Light Emission. *Inorg. Chem.* **2011**, *50*, 11323-11339.

(22) Kwon, J. E.; Park, S. Y. Advanced Organic Optoelectronic Materials: Harnessing Excited-State Intramolecular Proton Transfer (ESIPT) Process. *Adv. Mater.* **2011**, *23*, 3615-3642.

(23) Nano, A.; Gullo, M. P.; Ventura, B.; Armaroli, N.; Barbieri, A.; Ziessel, R. Panchromatic Luminescence from Julolidine Dyes Exhibiting Excited State Intramolecular Proton Transfer. *Chem. Commun.* **2015**, *51*, 3351-3354.

(24) Park, S.; Kwon, J. E.; Kim, S. H.; Seo, J.; Chung, K.; Park, S. Y.; Jang, D. J.; Medina, B. M.; Gierschner, J.; Park, S. Y. A White-Light-Emitting Molecule: Frustrated Energy Transfer between Constituent Emitting Centers. *J. Am. Chem. Soc.* **2009**, *131*, 14043-14049.

(25) Bronner, C.; Veiga, M.; Guenet, A.; De Cola, L.; Hosseini, M. W.; Strassert, C. A.; Baudron, S. A. Excited State Properties and Energy Transfer within Dipyrrin-Based Binuclear Iridium/Platinum Dyads: The Effect of ortho-Methylation on the Spacer. *Chem.-Eur. J.* **2012**, *18*, 4041-4050.

(26) Fanna, D. J.; Zhang, Y. J.; Li, L.; Karatchevtseva, I.; Shepherd, N. D.; Azim, A.; Price, J. R.; Aldrich-Wright, J.; Reynolds, J. K.; Li, F. 3d Transition Metal Complexes with a Julolidine-Quinoline Based Ligand: Structures, Spectroscopy and Optical Properties. *Inorg. Chem. Front.* **2016**, *3*, 286-295.

(27) Zhang, Y. J.; Fanna, D. J.; Shepherd, N. D.; Karatchevtseva, I.; Lu, K.; Kong, L. G.; Price, J. R. Dioxo-Vanadium(V), Oxo-Rhenium(V) and Dioxo-Uranium(Vi) Complexes with a Tridentate Schiff Base Ligand. *RSC Adv.* **2016**, *6*, 75045-75053.

(28) Borisov, S. M.; Saf, R.; Fischer, R.; Klimant, I. Synthesis and Properties of New Phosphorescent Red Light-Excitable Platinum(Ii) and Palladium(Ii) Complexes with Schiff Bases for Oxygen Sensing and Triplet-Triplet Annihilation-Based Upconversion. *Inorg. Chem.* **2013**, *52*, 1206-1216.

(29) Haidekker, M. A.; Theodorakis, E. A. Molecular Rotors - Fluorescent Biosensors for Viscosity and Flow. *Org. Biomol. Chem.* **2007**, *5*, 1669-1678.

(30) Lee, K. H.; Kim, S. M.; Kim, J. Y.; Kim, Y. K.; Yoon, S. S. Red Fluorescent Organic Light-Emitting Diodes Using Modified Pyran-containing DCJTB Derivatives. *Bull. Korean Chem. Soc.* **2010**, *31*, 2884-2888.

(31) Holt, J. J.; Calitree, B. D.; Vincek, J.; Gannon, M. K.; Detty, M. R. A Microwave-Assisted Synthesis of Julolidine-9-Carboxamide Derivatives and their Conversion to Chalcogenoxanthones via Directed Metalation. *J. Org. Chem.* **2007**, *72*, 2690-2693.

(32) Katritzky, A. R.; Rachwal, B.; Rachwal, S.; Abboud, K. A. Convenient Synthesis of Julolidines Using Benzotriazole Methodology. *J. Org. Chem.* **1996**, *61*, 3117-3126.

(33) Lee, K. H.; Park, M. H.; Kim, S. M.; Kim, Y. K.; Yoon, S. S. Modified Julolidine-Containing Emitters for Red Organic Light-Emitting Diodes. *Jpn. J. Appl. Phys.* **2010**, *49*, 08jg02.

(34) Dobkowski, J.; Wnuk, P.; Buczynska, J.; Pszona, M.; Orzanowska, G.; Frath, D.; Ulrich, G.; Massue, J.; Mosquera-Vazquez, S.; Vauthey, E.; Radzewicz, C.; Ziessel, R.; Waluk, J. Substituent and Solvent Effects on the Excited State Deactivation Channels in Anils and Boranils. *Chem.-Eur. J.* **2015**, *21*, 1312-1327.

(35) Frath, D.; Azizi, S.; Ulrich, G.; Retailleau, P.; Ziessel, R. Facile Synthesis of Highly Fluorescent Boranil Complexes. *Org. Lett.* **2011**, *13*, 3414-3417.

(36) Sonogashira, K. Development Of Pd-Cu Catalyzed Cross-Coupling of Terminal Acetylenes with sp(2)-Carbon Halides. *J. Organomet. Chem.* **2002**, *653*, 46-49.

(37) Benelhadj, K.; Massue, J.; Retailleau, P.; Ulrich, G.; Ziessel, R. 2-(2 '-Hydroxyphenyl)Benzimidazole and 9,10-Phenanthroimidazole Chelates and Borate Complexes: Solution- and Solid-State Emitters. *Org. Lett.* **2013**, *15*, 2918-2921.

(38) Ventura, B.; Barbieri, A.; Zanelli, A.; Barigelletti, F.; Seneclauze, J. B.; Diring, S.; Ziessel, R. Excited-State Dynamics in a Dyad Comprising Terpyridine-Platinum(II) Ethynylene Linked to Pyrrolidino-[60] Fullerene. *Inorg. Chem.* **2009**, *48*, 6409-6416.

(39) Williams, J. A. G. In *Photochemistry and Photophysics of Coordination Compounds Ii*; Balzani, V., Campagna, S., Eds. 2007; Vol. 281, p 205-268.

(40) Wong, K. M. C.; Yam, V. W. W. Luminescence Platinum(II) Terpyridyl Complexes - From Fundamental Studies to Sensory Functions. *Coord. Chem. Rev.* **2007**, *251*, 2477-2488.

(41) Colombo, M. G.; Brunold, T. C.; Riedener, T.; Gudel, H. U.; Fortsch, M.; Burgi, H. B. Facial Tris Cyclometalated Rh3+ And Ir3+ Complexes - Their Synthesis, Structure, And Optical Spectroscopic Properties. *Inorg. Chem.* **1994**, *33*, 545-550.

(42) King, K. A.; Spellane, P. J.; Watts, R. J. Excited-State Properties of a Triply Ortho-Metalated Iridium(Iii) Complex. *J. Am. Chem. Soc.* **1985**, *107*, 1431-1432.

(43) Flamigni, L.; Barbieri, A.; Sabatini, C.; Ventura, B.; Barigelletti, F. Photochemistry and Photophysics of Coordination Compounds: Iridium. *Top. Curr. Chem.* **2007**, *281*, 143-203.

(44) Montalti, M.; Credi, A.; Prodi, L.; Gandolfi, M. T. *Handbook of Photochemistry*; 3rd ed.; CRC Press, Taylor & Francis: Boca Raton, FL, USA, 2006.

(45) Lakowicz, J. R. *Principles of Fluorescence Spectroscopy*; 3rd ed.; Springer: New York, USA, 2006.

(46) Ventura, B.; Barbieri, A.; Barigelletti, F.; Diring, S.; Ziessel, R. Energy Transfer Dynamics in Multichromophoric Arrays Engineered from Phosphorescent Pt-II/Ru-II/Os-II Centers Linked to a Central Truxene Platform. *Inorg. Chem.* **2010**, *49*, 8333-8346.

(47) Schanda, J. In *Colorimetry: Understanding the Cie System*; Schanda, J., Ed.; John Wiley & Sons, Inc.: Hoboken, NJ, USA, 2007, p 25-78.

(48) Yip, H. K.; Cheng, L. K.; Cheung, K. K.; Che, C. M. Luminescent Platinum(Ii) Complexes - Electronic Spectroscopy of Platinum(Ii) Complexes of 2,2' 6',2"-Terpyridine (Terpy) and p-Substituted Phenylterpyridines and Crystal-Structure of Pt(Terpy)Cl CF3SO3. *J. Chem. Soc.-Dalton Trans.* **1993**, 2933-2938.

(49) Dangles, O.; Guibe, F.; Balavoine, G.; Lavielle, S.; Marquet, A. Selective Cleavage of the Allyl and Allyloxcarbonyl Groups Through Palladium-Catalyzed Hydrostannolysis with Tributyltin Hydride - Application to the Selective Protection-Deprotection of Amino-Acid Derivatives and in Peptide-Synthesis. *J. Org. Chem.* **1987**, *52*, 4984-4993.

(50) Lee, C. C.; Hu, A. T. Synthesis and Optical Recording Properties of Some Novel Styryl Dyes for DVD-R. *Dyes Pigment.* **2003**, *59*, 63-69.

SYNOPSIS TOC. The introduction of an N^O chelating site onto a julolidine dyes has allowed the synthesis of a series of luminescent metal complexes and arrays. The **PtIrL$_3$** system display an excitation wavelength dependent emission that allows the generation of pure and warm white color.